Soft Matter

Cite this: *Soft Matter*, 2011, **7**, 5854

www.rsc.org/softmatter

PAPER

Enhancement of DNA compaction by negatively charged nanoparticles. Application to reversible photocontrol of DNA higher-order structure†

Sergii Rudiuk,‡[a] Kenichi Yoshikawa[a] and Damien Baigl*[bcd]

Received 22nd February 2011, Accepted 11th April 2011
DOI: 10.1039/c1sm05314k

We report for the first time that negatively charged silica nanoparticles (NPs) enhance the ability of cationic surfactants to induce genomic DNA compaction. Single-chain compaction of duplex DNA molecules was studied by fluorescence microscopy in the presence of dodecyltrimethylammonium bromide (DTAB) and NPs. We found that very small amounts of NPs ($\sim 10^{-4}$ to 10^{-2} wt%) significantly decreased the concentration of the surfactant at which DNA is compacted. This effect was maximal at intermediate NP concentration (here, 1.5×10^{-3} wt%) where the concentration of DTAB necessary for DNA compaction was 5-fold smaller than that in the absence of NPs. As a possible mechanism, we suggest that negatively charged NPs, by inducing the aggregation of DTAB molecules through electrostatic interactions, promote cooperative binding to DNA and thus enhance the ability of DTAB to compact DNA. By applying this phenomenon to a photosensitive cationic surfactant (AzoTAB), we could achieve reversible control of DNA higher-order structure using light at a much lower AzoTAB concentration than what has been reported up to now.

Introduction

Controlling DNA higher-order structure is important for various fundamental studies and applications,[1] such as DNA-based nanomaterials design[2–4] and control of biological activity.[5] DNA is a negatively charged polyelectrolyte and its compaction is usually achieved either by charge neutralization using cationic agents such as polyamines,[6,7] surfactants,[8,9] nanoparticles[10,11] or by creating unfavorable contacts with the solvent (PEG,[12] precipitation in alcohol,[13] low dielectric constant,[14] *etc.*). However, to our knowledge, the effect of negatively charged nanoparticles (NPs) on DNA compaction has never been studied.

Recently a breakthrough has been realized with the possibility to control DNA higher-order structure using light.[15–17] A photosensitive, azobenzene trimethylammonium bromide surfactant (AzoTAB) (Fig. 1) was used for this purpose. When irradiated at 365 nm this surfactant undergoes a *trans* to *cis* isomerization accompanied by a change of polarity.[18] Consequently, there exists an AzoTAB concentration range for which DNA is compacted under dark conditions but unfolded under UV illumination at 365 nm. Thus, the decompaction of nucleic acid can be achieved by UV irradiation of DNA–AzoTAB complexes. However, the activity of AzoTAB to compact DNA is low, that is, a high concentration of surfactant is necessary to achieve the compaction and light-induced decompaction, which can be a limitation for applications due to AzoTAB cytotoxicity at a high concentration. When another photosensitive agent with a much higher affinity for DNA has been used, DNA compaction could be achieved at a very low surfactant concentration but it was not reversible anymore.[17,19] Thus, finding conditions for increasing AzoTAB affinity for DNA while keeping reversible the photocontrol of DNA higher-order structure is an important challenge.

Here, we studied for the first time the effect of negatively charged silica nanoparticles (NPs) in the compaction of DNA by

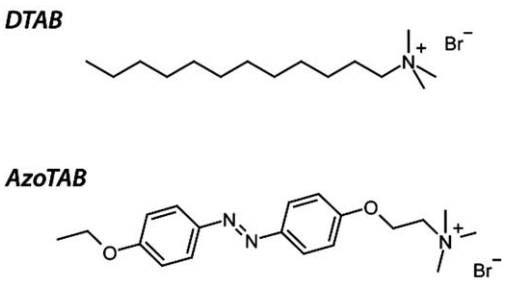

Fig. 1 Structures of DTAB and AzoTAB.

[a]*Department of Physics, Graduate School of Science, Kyoto University, Kyoto, 606-8502, Japan*
[b]*Department of Chemistry, Ecole Normale Supérieure, 75005 Paris, France. E-mail: damien.baigl@ens.fr; Fax: +33 1 4432 2402; Tel: +33 1 4432 243*
[c]*Université Pierre et Marie Curie Paris 6, 75005 Paris, France*
[d]*UMR 8640, CNRS, France*

† Electronic supplementary information (ESI) available: Fig. S1. Effect of surfactant hydrophobic chain length on enhancement of DNA compaction. See DOI: 10.1039/c1sm05314k

‡ Present address: Department of Chemistry, Ecole Normale Supérieure, 75005 Paris, France.

cationic surfactants: dodecyltrimethylammonium bromide (DTAB) as a standard surfactant and AzoTAB as a photosensitive one (Fig. 1). These two surfactants have the same cationic polar head and a similar hydrophobicity (critical micellar concentrations (CMC) are 15.5 mM[20] and 12.6 mM[17] in pure water at 25 °C for DTAB and AzoTAB, respectively). We found for the first time that the presence of NPs at very low concentrations ($\sim 10^{-4}$ to 10^{-2} wt%) enhances the activity of both surfactants to compact DNA.

In the case of AzoTAB, this enhancement was compatible with reversible photocontrol of DNA higher-order structure. In such a system, DNA could thus be reversibly compacted and unfolded using light in a medium containing a relatively low concentration of AzoTAB and a very small amount of NPs.

Results and discussion

Negatively charged particles enhance the ability of cationic surfactants to induce DNA compaction

To study the effect of negatively charged nanoparticles, we chose 100 nm silica nanoparticles for their colloidal stability, biocompatibility,[21,22] and low damage to DNA, contrary to TiO_2 or ZnO nanoparticles, which are known to induce oxidative damage to DNA,[23,24] especially under UV illumination.[23] First, we observed that for a given concentration of DTAB, the addition of very low amounts (10^{-4}–10^{-2} wt%) of 100 nm anionic silica NPs increased its ability to compact DNA. In order to investigate this phenomenon, we studied the compaction of DNA by DTAB in the presence and in the absence of a fixed concentration of NPs (1.5×10^{-3} wt%) by fluorescence microscopy. Using this method, a large number of individual DNA molecules can be observed and their higher-order structure (coil or compact state) can be assessed. Without DTAB, all DNA molecules are in the coil state regardless of the presence or absence of NPs (Fig. 2, left). With a moderate increase in DTAB concentration, no significant evolution in the higher-order structure of DNA molecules is observed in the absence of NPs. In contrast, in the presence of NPs, an increasing fraction of DNA molecules in the compact state is observed. For instance, at [DTAB] = 300 μM, 0% and 99% of DNA molecules are in the compact state in the absence and in the presence of NPs, respectively (Fig. 2, middle). With a further increase in DTAB concentration, the fraction of DNA molecules in the compact state increases, even in the absence of NPs. At [DTAB] = 1000 μM, all DNA molecules are in the compact state regardless of the presence or absence of NPs (Fig. 2, right). These observations demonstrate that the presence of a very small amount of NPs (here, 1.5×10^{-3} wt%) enhances the activity of DTAB to compact DNA.

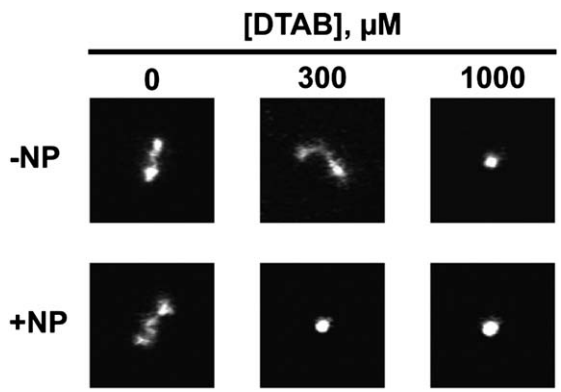

Fig. 2 Enhancement of DTAB-induced DNA compaction by 100 nm silica nanoparticles (NPs). Typical fluorescence microscopy images of DNA molecules in solution for various DTAB concentrations, in the absence (−NP) and in the presence (+NP) of 100 nm silica nanoparticles (NPs). Each image has a size 5 μm × 5 μm. [DNA] = 0.1 μM; [YOYO] = 0.01 μM; [NPs] = 1.5×10^{-3} wt%; [Tris/HCl] = 10 mM (pH = 7.4).

Effect of NP concentration

Next we studied the effect of NP concentration on the enhancement of DNA compaction. Fig. 3 shows compaction curves, that is, the percentage of DNA molecules in the compact state as a function of DTAB concentration, for several NP concentrations. Regardless of NP concentration, all compaction curves have a sigmoidal shape, which is a typical observation in DNA–surfactant systems and a signature of a cooperative process.[17,25,26] Fig. 3A shows that, at low NP concentrations, the

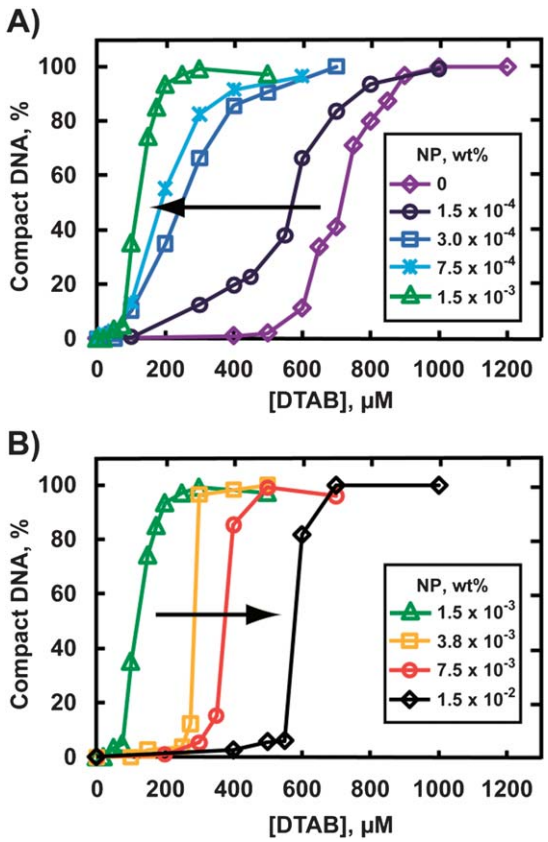

Fig. 3 Effect of NP concentration on DTAB-induced DNA compaction. Percentage of DNA molecules in the compact state as a function of DTAB concentration for various NP concentrations: (A) 0–1.5×10^{-3} wt %; (B) 1.5×10^{-3}–1.5×10^{-2} wt%. Symbols are data points. Lines connecting symbols are guides for the eyes. Black arrows indicate an increasing concentration of NPs. [DNA] = 0.1 μM; [YOYO] = 0.01 μM; [Tris/HCl] = 10 mM (pH = 7.4).

increase of the amount of NPs in the solution leads to a gradual shift of compaction curves toward low DTAB concentrations. Let [$DTAB_{50}$] be the concentration of DTAB corresponding to 50% of DNA molecules in the compact state. [$DTAB_{50}$] decreases from 715 μM to 120 μM with an increase in NP concentration from 0 to 1.5×10^{-3} wt%. Notably, Fig. 3B shows that a further increase in NP concentration results in the opposite trend. In this NP concentration range, [$DTAB_{50}$] increases from 120 μM to 585 μM with an increase in NP concentration from 1.5×10^{-3} wt% to 1.5×10^{-2} wt%. The effect of NP concentration is summarized in Fig. 4 where the ratio $R = [DTAB_{50}]/[DTAB_{50}^*]$ ([$DTAB_{50}^*$] is the DTAB concentration to achieve 50% of DNA compaction in the absence of NPs) is plotted as a function of NP concentration. Fig. 4 shows that the presence of NPs enhances the ability of DTAB to induce DNA compaction in all the ranges of NP concentration used in this study (from 1.5×10^{-4} wt% to 1.5×10^{-2} wt%). Moreover an optimum enhancement of DTAB-induced DNA compaction is observed for a NP concentration around 1.5×10^{-3} wt%. It can be noted that this concentration of NPs corresponds to 72.3 NPs per T4 DNA molecule on average. This figure corresponds to approximately 736.4 nm of DNA per nanoparticle, which is about 2.3 times the NP circumference (314 nm). All these results show that NPs participate in compaction of DNA and provide some indications on the possible mechanism of the enhancement of DNA compaction. We hypothesize that NPs act as nucleation sites for the aggregation of surfactants through electrostatic interactions between the NP's negatively charged surface and surfactant cationic heads. It has been well established from the seminal studies of Hayakawa *et al.* that the binding of cationic surfactants to DNA is highly cooperative.[25] As a consequence, any physico-chemical parameter that favors the aggregation of surfactants enhances the possibility of the surfactant molecules to cooperatively bind to DNA and therefore promotes DNA compaction at a lower surfactant concentration. This effect is observed for instance when the hydrophobicity of the surfactant apolar tail is increased.[9,17,26] Here, nanoparticles can promote the aggregation of DTAB molecules through electrostatic attraction and therefore enhance the ability of DTAB to induce DNA compaction. The existence of an optimal NP concentration to get this enhancement can be explained as follows. At low NP concentrations, the concentration of nucleation sites is small and the cooperative effects are limited. With an increase in NP concentration, the concentration of nucleation sites increases and the enhancement in DNA compaction becomes larger. This holds true as long as the number of aggregated surfactants per nanoparticle is maximal. When NP concentration becomes too large, surfactants can still interact with the NPs but the number of aggregated surfactants per nanoparticle decreases and effects of cooperativity weaken. With a further increase in NP concentration, this 'dilution' effect increases thus decreasing the ability of DTAB to induce compaction. The electrostatic interaction between DTAB and negatively charged NPs was characterized by ζ potential measurements. Fig. 5 shows zeta potential ζ of the nanoparticles as a function of [DTAB] for a concentration of NPs fixed at the optimal value (1.5×10^{-3} wt%). It shows that ζ increases from about -27 ± 3 mV, the value for bare silica NPs, up to positive values when DTAB is progressively added to the solution. This observation indicates that DTAB molecules electrostatically adsorb on the negatively charged surface of NPs, forming a monolayer onto which additional DTAB molecules can adsorb by hydrophobic interactions. Similar phenomenon has been reported with the cationic surfactant cetyltrimethylammonium bromide (CTAB), which was shown to form bilayers or multilayers on silica NPs and induced a change of ζ from −34 mV to +(37–54) mV.[27] Notably, our results show that the neutralization of silica NPs ($\zeta = 0$) takes place at a concentration of DTAB higher than that corresponding to full compaction of DNA. This shows that DNA compaction is not induced by NPs overcharged by an excess of DTAB but by DTAB molecules adsorbed on NPs which act cooperatively with better efficiency than individual DTAB molecules from the bulk solution. Finally, to study whether the surfactant–nanoparticle

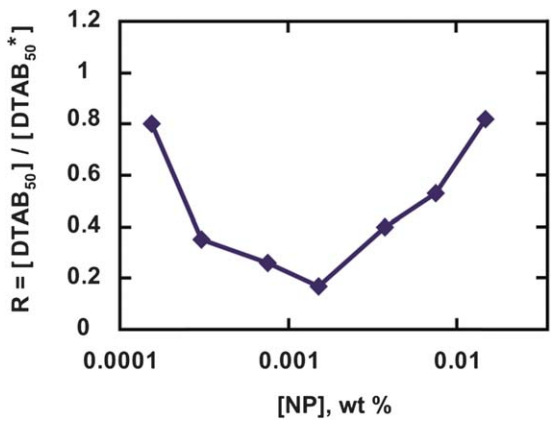

Fig. 4 Effect of NP concentration on the enhancement of DNA compaction by DTAB. Ratio R of surfactant concentration corresponding to 50% of DNA compaction in the presence ([$DTAB_{50}$]) and in the absence ([$DTAB_{50}^*$]) of NPs as a function of NP concentration. Symbols are data points. Lines connecting symbols are guides for the eyes. [DNA] = 0.1 μM; [YOYO] = 0.01 μM; [Tris/HCl] = 10 mM (pH = 7.4).

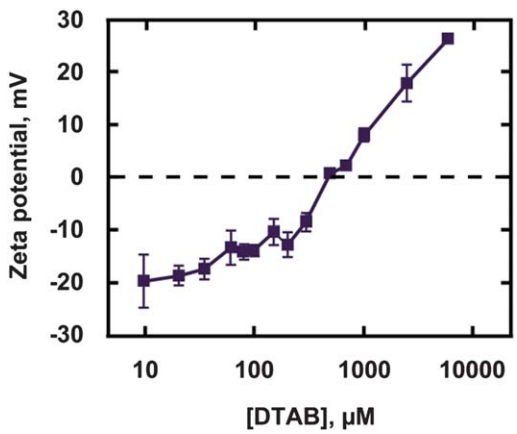

Fig. 5 Effect of DTAB on the ζ potential of NPs. ζ Potential of NPs as a function of DTAB concentration. Symbols are data points. Lines connecting symbols are guides for the eyes. Error bars show the standard deviations observed on three replicates. [NPs] = 1.5×10^{-3} wt%; [Tris/HCl] = 10 mM (pH = 7.4).

interaction is mainly of electrostatic or hydrophobic nature, we systematically studied the effect of surfactant chain length on DNA compaction enhancement by the nanoparticles. ESI, Fig. S1† shows the enhancement of DNA compaction as a function of NP concentration for three cationic surfactants having the same cationic charge but different number of carbon atoms n in the hydrophobic tail: DTAB ($n = 12$), TTAB ($n = 14$), and CTAB ($n = 16$). It shows that, regardless of n, the maximum enhancement is obtained for a similar NP concentration ([NP] = 1.5×10^{-3} wt%). Moreover, the enhancement amplitude significantly decreases with an increase in n, that is, in surfactant hydrophobicity. These results show that the enhancement of DNA compaction is mainly due to the aggregation of cationic surfactants on negatively charged NPs through electrostatic interactions and not hydrophobic interactions. We thus conclude that negatively charged NPs, by inducing the aggregation of DTAB molecules through electrostatic interactions, promote cooperative binding to DNA and thus enhance the ability of DTAB to compact DNA. This enhancement is maximal for an intermediate concentration of NPs, which corresponds to optimal aggregation of DTAB molecules on the nanoparticles.

Enhancement of photocontrolled DNA compaction by NPs

Then, we applied this phenomenon to improve reversible control of DNA higher-order structure using light. Recently, we demonstrated that the use of a photosensitive cationic surfactant, called AzoTAB, can be used to control DNA higher-order structure using light in bulk as well as in cell-mimicking microenvironments.[16] Such a method is particularly interesting because we have shown that these light-induced conformational changes of DNA can be applied for the reversible photocontrol of gene expression systems at both transcription and translation levels.[5] AzoTAB has a molecular structure similar to DTAB but its hydrophobic tail contains a photosensitive azobenzene group (Fig. 1). Under dark conditions, the photostable isomer is mainly *trans*-AzoTAB, which has a maximum absorption at about $\lambda_{max} = 356$ nm. Under UV illumination at 365 nm, AzoTAB undergoes an isomerization into *cis*-AzoTAB ($\lambda_{max}^{1} = 320$ nm, $\lambda_{max}^{2} = 440$ nm). Under conditions of DNA observation (10 mM Tris–HCl buffer), *trans* to *cis* isomerization is complete after about 1 min of UV exposure. *Cis* to *trans* isomerization can be achieved by exposure to visible light. Both *trans*-AzoTAB and *cis*-AzoTAB are stable isomers and no evolution is observed when samples are kept in the dark for a few hours at room temperature. First, we studied the compaction of DNA by AzoTAB (*trans* isomer) in the presence and in the absence of the optimal concentration of NPs (1.5×10^{-3} wt%) by fluorescence microscopy (Fig. 6). Similar to the observations made with DTAB (Fig. 2), without AzoTAB, all DNA molecules are in the coil state regardless of the presence or absence of NPs (Fig. 6A, left). With a moderate increase in AzoTAB concentration, no significant evolution in the higher-order structure of DNA molecules is observed in the absence of NPs. In contrast, in the presence of NPs, an increasing fraction of DNA molecules in the compact state is observed. For instance, at [AzoTAB] = 200 μM, 2% and 87% of DNA molecules are in the compact state in the absence and in the presence of NPs, respectively (Fig. 6A, middle). With a further increase in AzoTAB concentration, the

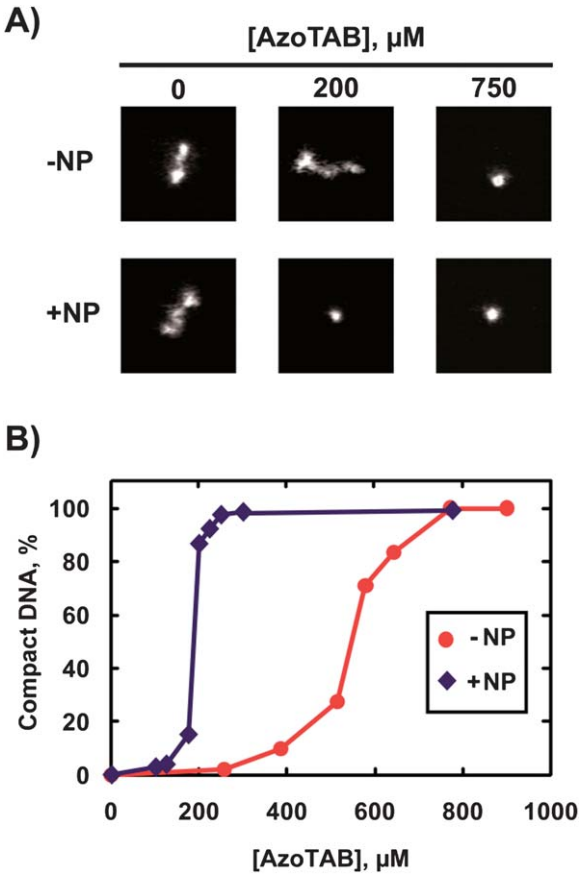

Fig. 6 Enhancement of AzoTAB-induced DNA compaction by NPs. (A) Typical fluorescence microscopy images of DNA molecules in solution for various AzoTAB concentrations, in the absence (−NP) or in the presence (+NP) of silica nanoparticles. Each image has a size 5 μm × 5 μm. (B) Percentage of DNA molecules in the compact state as a function of AzoTAB concentration, in the absence (−NP) or in the presence (+NP) of silica nanoparticles. Symbols are data points. Lines connecting symbols are guides for the eyes. [DNA] = 0.1 μM; [YOYO] = 0.01 μM; [NPs] = 1.5×10^{-3} wt%; [Tris/HCl] = 10 mM (pH = 7.4).

fraction of DNA molecules in the compact state increases, even in the absence of NPs. At [AzoTAB] = 750 μM, all DNA molecules are in the compact state regardless of the presence or absence of NPs (Fig. 6A, right). Fig. 6B shows the compaction curves as a function of AzoTAB concentration, with and without NPs (1.5×10^{-3} wt%). Similar to what has been observed with DTAB, Fig. 6B shows that NPs greatly enhance the ability of AzoTAB to induce DNA compaction. For instance, 50% of DNA compaction is achieved for [$AzoTAB_{50}$*] = 550 μM and [$AzoTAB_{50}$] = 185 μM, in the absence and in the presence of NPs, respectively. This corresponds to a 3-fold enhancement of AzoTAB ability to compact DNA.

Reversible photocontrol of DNA higher-order structure in the presence of NPs

Then, we studied the effect of light illumination on compaction of DNA by AzoTAB in the presence of NPs. Fig. 7 shows DNA compaction curves as a function of [AzoTAB] in the presence of a fixed concentration of NPs (1.5×10^{-3} wt%), with (+UV) or

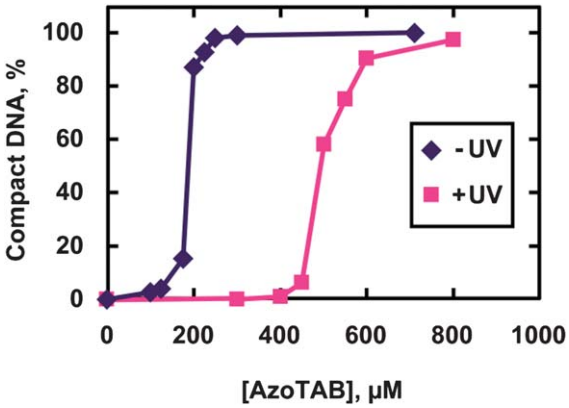

Fig. 7 Effect of UV illumination in the presence of silica nanoparticles. Percentage of DNA molecules in the compact state as a function of AzoTAB concentration, in the presence of silica nanoparticles with (+UV) and without (−UV) illumination at 365 nm for 3 min. Symbols are data points. Lines connecting symbols are guides for the eyes. [DNA] = 0.1 μM; [YOYO] = 0.01 μM; [NPs] = 1.5×10^{-3} wt%; [Tris/HCl] = 10 mM (pH = 7.4).

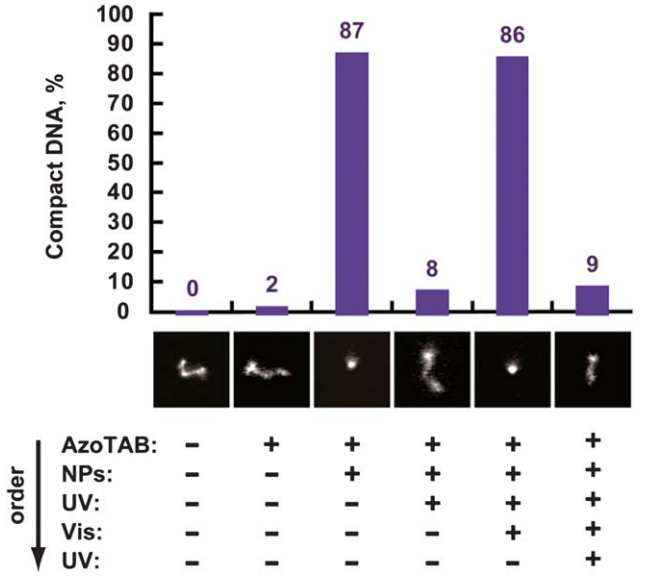

Fig. 8 Photoreversible DNA compaction in the presence of NPs. Percentage of DNA molecules in the compact state (top) and typical fluorescence microscopy images of DNA (middle) with or without each following operation (bottom), in this order: (1) addition of AzoTAB; (2) addition of NPs; (3) illumination at 365 nm for 3 min; (4) exposure to visible light for 3 hours; and again (5) illumination at 365 nm for 3 min. Each image has a size 5 μm × 5 μm. [DNA] = 0.1 μM; [YOYO] = 0.01 μM; [AzoTAB] = 200 μM; [NPs] = 1.5×10^{-3} wt%; [Tris/HCl] = 10 mM (pH = 7.4).

without (−UV) UV illumination (3 min at 365 nm). For this experiment, UV illumination is applied *before* NP and DNA introduction, which means that −UV and +UV curves correspond to DNA compaction by mainly *trans*-AzoTAB and *cis*-AzoTAB, respectively. Fig. 7 clearly shows that *trans* and *cis* isomers have different abilities to induce DNA compaction. 50% of DNA compaction is achieved at [$AzoTAB_{50}$] = 185 μM and 490 μM, in the absence and in the presence of UV illumination, respectively. This difference can be interpreted by the difference in the polarity of the hydrophobic tail between *trans* and *cis* isomers. *Trans*-AzoTAB being less polar than *cis*-AzoTAB, it has thus a lower CMC (12.6 mM and 14.6 mM for *trans*-AzoTAB and *cis*-AzoTAB, respectively[17]), a greater propensity to form aggregates and therefore a greater ability to induce DNA compaction through cooperative binding. Interestingly, in the absence of NPs, we found [$AzoTAB_{50}$*] = 550 μM and 885 μM (data not shown) in the absence and in the presence of UV illumination, respectively. All these results demonstrate that the presence of NPs does not affect the effect of UV illumination on DNA compaction. Therefore, the AzoTAB–NP system allows one to achieve photo-dependent compaction of DNA at an AzoTAB concentration that is approximately 3 times lower than that in the absence of NPs.

A crucial parameter for photoswitchable DNA compaction systems is the reversibility of DNA conformational transitions upon illumination. For instance, it has been shown that a too strong DNA affinity of the photosensitive compaction agent can decrease the capacity of unfolding DNA by light.[17,19] To assess the photo-reversibility of the DNA–NP system, we first added AzoTAB (200 μM) and NPs (1.5×10^{-3} wt%) to the DNA solution to get most of the DNA molecules in the compact state. We then applied successive illumination conditions *on the same solution* and we characterized the conformational state of a large number of individual DNA molecules by fluorescence microscopy. Fig. 8 shows the fraction of DNA molecules in the compact state for these successive conditions. In the presence of only AzoTAB or NPs, most of the DNA molecules stay in the unfolded state (2% and 0% of DNA molecules in the compact state, respectively). In contrast, when both agents were used simultaneously, the majority of DNA molecules (87%) were in the compact state. These observations confirm the synergy between AzoTAB and NPs to induce DNA compaction. Then, UV (365 nm) was applied on this solution for 3 min. We observed that most of the DNA molecules have been unfolded (8% of compact state). Then, when visible light was applied on the same solution, we observed that most of the DNA molecules have folded back to the compact state (86% of compact state). When UV irradiation was repeated one more time, most of the DNA molecules were unfolded again (9% of compact state). This shows that the compaction of DNA by AzoTAB–NP system is fully reversible upon illumination and several cycles of compaction/unfolding can be obtained in a given DNA solution by successive visible/UV light illumination. We have thus successfully built a system allowing us (i) to compact DNA at a relatively low concentration of AzoTAB (approx. 3 times smaller than that under classical conditions, that is, in the absence of NPs); and (ii) to induce reversible DNA unfolding/folding transition by application of UV/visible light illumination.

Materials and methods

Materials

Bacteriophage T4 DNA (166 kbp) was from Wako Chemicals, YOYO-1 iodide was from Molecular Probes. DTAB was from TCI (Tokyo, Japan). Silica nanoparticles (100 nm diameter) were a gift from Nissan Chemicals. All other chemicals were from

Sigma. Deionised water (Millipore, 18 MΩ cm^{-1}) was used for all experiments.

AzoTAB synthesis

Azobenzene trimethylammonium bromide (AzoTAB) synthesis was adapted from the method described by Hayashita *et al.*[28] A detailed protocol of the homolog synthesis can be found in ref. 17.

Preparation of DNA samples

Water, Tris–HCl buffer, surfactant (DTAB or AzoTAB), 100 nm silica nanoparticles (NPs), and YOYO-1 iodide were mixed in this order prior to careful T4 DNA introduction (under low shear conditions to avoid DNA breakage[29]). In order to permit the efficient adsorption of the surfactant on the nanoparticles, the samples were equilibrated for 15 min after vigorous mixing of the surfactant with the NPs. After addition of YOYO and DNA, the samples were equilibrated for a second time for 15 min prior to observation of the nucleic acid by fluorescence microscopy. Equilibrium steps before and after DNA introduction were systematically applied to get reproducible data. For compaction curves using *cis*-AzoTAB, a solution of AzoTAB in Tris/HCl buffer was irradiated at 365 nm for 3 minutes before the addition of silica NPs. For all experiments, we used T4 DNA at a final concentration of 0.1 μM (concentration in nucleotides) in Tris–HCl buffer (10 mM, pH 7.4) with YOYO (0.01 μM) as a DNA fluorescent dye. In the case of AzoTAB, for all steps except UV illuminations, DNA samples were kept under dark conditions. All experiments were performed at room temperature.

UV and visible light illumination

UV exposure was performed by placing the corresponding samples containing AzoTAB for 3 min at 6 cm distance from an 8 W UVLMS-38 UV lamp (UVP, Upland, CA) working at 365 nm. According to the measurements of DNA size[16] and biological activity,[5] UV illumination at 365 nm does not induce significant damage to DNA under these conditions. In order to expose the solutions to visible light, they were placed for this study for 3 hours at 50 cm distance from a 60 W incandescent lamp. Note that this exposure time can be strongly decreased if a light source with more power in blue is used (1 min exposure is sufficient in the case of a 100 W mercury lamp equipped with a 400 nm longpass filter[5]).

Fluorescence microscopy (FM)

Fluorescence microscopy was performed using an Axiovert 135 TV (Zeiss) microscope equipped with a 100× oil-immersion lens. Images were recorded using an EB-CCD camera and an image processor Argus 10 (Hamamatsu Photonics). DNA molecules stained with YOYO were observed in 20 μL microdroplets deposited on a clean glass cover slide. Under these conditions the compaction states of DNA are clearly distinguishable: DNA molecules in the compact state appear as bright fast-diffusing spots, whereas DNA molecules in the coil state have a much larger apparent long-axis length, a much lower translational diffusion coefficient and exhibit characteristic intra-chain thermal fluctuations. For each observation, a minimum of 150 individual DNA molecules were characterized to determine the fraction of molecules in the compact state. All experiments were performed at room temperature.

ζ Potential measurements

ζ Potential of silica nanoparticles was measured with Zetasizer Nano-ZS (Malvern Instruments) at 25 °C. Mixtures of silica NPs (final concentration: 1.5×10^{-3} wt%) and increasing amounts of DTAB were prepared in 10 mM Tris/HCl buffer (pH 7.4). After mixing, the samples were equilibrated for 15 min at room temperature prior to ζ potential measurements. Each measurement was repeated 10 times. The changes in mean ζ potential were then plotted against DTAB concentration.

Conclusions

We have studied DNA compaction by both standard and photosensitive cationic surfactants in the presence of anionic silica nanoparticles (NPs), and found that the presence of NPs enhances the ability of surfactants to induce DNA compaction. Our results indicate that negatively charged NPs, by inducing the aggregation of cationic surfactant molecules, promote cooperative binding to DNA and thus enhance the ability of these surfactants to compact DNA. This enhancement is maximal for an intermediate concentration of NPs, which corresponds to optimal aggregation of DTAB molecules on the nanoparticles. By using a photosensitive surfactant, AzoTAB, we have built a system allowing the reversible photocontrol of DNA higher-order structure at a relatively low concentration of photosensitive surfactant. This can be particularly interesting for applications. For instance, it has been established that photo-induced DNA conformational changes can be used to control using light biological reactions such as transcription and translation.[5] However, the concentration of AzoTAB needed in the classical conditions to achieve the photocontrol is high (~1 to 2 mM). Here, photocontrol has been proved efficient and reversible at concentrations down to ~200 μM. Our system could thus be developed for low-invasive photocontrol of gene expression systems.

Acknowledgements

The research leading to these results has received funding from the Japan Science and Technology Agency under the ICORP 2006 "Spatio-Temporal Order" project, the Institut Universitaire de France, and the European Research Council under the European Community's Seventh Framework Programme (FP7/2007-2013) / ERC Grant agreement n 258782.

References

1 A. Estévez-Torres and D. Baigl, *Soft Matter*, 2011, DOI: 10.1039/c1sm05373f.
2 P. W. K. Rothemund, *Nature*, 2006, **440**, 297.
3 Y. Y. Pinto, J. D. Le, N. C. Seeman, K. Musier-Forsyth, T. A. Taton and R. A. Kiehl, *Nano Lett.*, 2005, **5**, 2399.
4 A. A. Zinchenko, K. Yoshikawa and D. Baigl, *Adv. Mater.*, 2005, **17**, 2820.

5 A. Estévez-Torres, C. Crozatier, A. Diguet, T. Hara, H. Saito, K. Yoshikawa and D. Baigl, *Proc. Natl. Acad. Sci. U. S. A.*, 2009, **106**, 12219.
6 L. C. Gosule and J. A. Schellman, *Nature*, 1976, **259**, 333.
7 D. Baigl and K. Yoshikawa, *Biophys. J.*, 2005, **88**, 3486.
8 S. M. Mel'nikov, V. G. Sergeyev and K. Yoshikawa, *J. Am. Chem. Soc.*, 1995, **117**, 2401.
9 S. Rudiuk, S. Franceschi-Messant, N. Chouini-Lalanne, E. Perez and I. Rico-Lattes, *Langmuir*, 2008, **24**, 8452.
10 A. A. Zinchenko, K. Yoshikawa and D. Baigl, *Phys. Rev. Lett.*, 2005, **95**, 228101.
11 A. A. Zinchenko, T. Sakaue, S. Araki, K. Yoshikawa and D. Baigl, *J. Phys. Chem.*, 2007, **111**, 3019.
12 U. K. Laemmli, *Proc. Natl. Acad. Sci. U. S. A.*, 1975, **72**, 4288.
13 K. B. Roy, T. Antony, A. Saxena and H. B. Bohidar, *J. Phys. Chem. B*, 1999, **103**, 5117.
14 S. M. Mel'nikov, M. O. Khan, B. Lindman and B. Jönsson, *J. Am. Chem. Soc.*, 1999, **121**, 1130.
15 A.-L. M. Le Ny and C. T. Lee, Jr, *J. Am. Chem. Soc.*, 2006, **128**, 6400.
16 M. Sollogoub, S. Guieu, M. Geoffroy, A. Yamada, A. Estévez-Torres, K. Yoshikawa and D. Baigl, *ChemBioChem*, 2008, **9**, 1201.
17 A. Diguet, N. K. Mani, M. Geoffroy, M. Sollogoub and D. Baigl, *Chem.–Eur. J.*, 2010, **6**, 11890.
18 A. Diguet, R.-M. Guillermic, N. Magome, A. Saint-Jalmes, Y. Chen, K. Yoshikawa and D. Baigl, *Angew. Chem., Int. Ed.*, 2009, **48**, 9281.
19 M. Geoffroy, D. Faure, R. Oda, D. M. Bassani and D. Baigl, *ChemBioChem*, 2008, **9**, 2382.
20 R. Sabaté, M. Gallardo and J. Estelrich, *Electrophoresis*, 2000, **21**, 481.
21 I. I. Slowing, B. G. Trewyn, S. Giri and V. S.-Y. Lin, *Adv. Funct. Mater.*, 2007, **17**, 1225.
22 C. A. Barnes, A. Elsaesser, J. Arkusz, A. Smok, J. Palus, A. Leśniak, A. Salvati, J. P. Hanrahan, W. H. de Jong and E. Dziubałtowska, et al., *Nano Lett.*, 2008, **8**, 3069.
23 R. Dunford, A. Salinaro, L. Cai, N. Serpone, S. Horikoshi, H. Hidaka and J. Knowland, *FEBS Lett.*, 1997, **418**, 87.
24 F. Afaq, P. Abidi, R. Matin and Q. Rahman, *J. Appl. Toxicol.*, 1998, **18**, 307.
25 K. Hayakawa, J. P. Santerre and J. C. T. Kwak, *Biophys. Chem.*, 1983, **17**, 175.
26 R. Dias, S. Mel'nikov, B. Lindman and M. G. Miguel, *Langmuir*, 2000, **16**, 9577.
27 E. Yu. Bryleva, N. A. Vodolazkaya, N. O. McHedlov-Petrossyan, L. V. Samokhina, N. A. Matveevskaya and A. V. Tolmachev, *J. Colloid Interface Sci.*, 2007, **316**, 712.
28 T. Hayashita, T. Kurosawa, T. Miyata, K. Tanaka and M. Igawa, *Colloid Polym. Sci.*, 1994, **272**, 1611.
29 L. Cinque, Y. Ghomchi, Y. Chen, A. Bensimon and D. Baigl, *ChemBioChem*, 2010, **11**, 340.

